Uncertainty Analysis of System Identification Results Obtained for a Seven Story Building Slice Tested on the UCSD-NEES Shake Table

Babak Moaveni[1], Andre R. Barbosa[2], Joel P. Conte[3], and François M. Hemez[4]

ABSTRACT

A full-scale seven-story reinforced concrete building section/slice was tested on the NEES shake table at the University of California San Diego during the period of October 2005 to January 2006. Three output-only system identification methods were used to extract the modal parameters (natural frequencies, damping ratios, and mode shapes) of the test structure at different damage states. In this study, the performance of these system identification methods is investigated in two cases: (Case I) when these methods are applied to the measured dynamic response of the structure, and (Case II) when these methods are applied to the dynamic response of the structure simulated using a three-dimensional nonlinear finite element model thereof. In both cases, the uncertainty/variability of the identified modal parameters due to the variability of several input factors is quantified through analysis-of-variance (ANOVA). In addition to ANOVA, meta-models are used for effect screening in Case II (based on the simulated data) which also capture the effects of linear interactions of the input factors. The four input factors considered in Case I are: amplitude of input excitation, spatial density of measurements, length of response data used for system identification, and model order used in the parametric system identification methods. In the second case of uncertainty analysis, in addition to these four input factors, measurement noise is also considered. The results show that for all three methods considered, amplitude of excitation is the most significant factor explaining the variability of the identified modal parameters, especially the natural frequencies.

Key Words: System identification, variability in modal parameters, uncertainty quantification

[1] Corresponding author. Assistant Professor, Dept. of Civil and Environmental Engineering, Tufts University, Medford, MA 02155. Telephone: 617-627-5642; Fax: 617-627-3994; Email: babak.moaveni@tufts.edu.

[2] Assistant Professor, School of Civil and Construction Engineering, Oregon State University, Corvallis.

[3] Professor, Dept. of Structural Engineering, University of California, San Diego.

[4] XCP 1-Division, Los Alamos National Laboratory, New Mexico.

1. Introduction

In recent years, structural health monitoring has gained increased interest and attention from the civil engineering community as a potential tool to identify damage at its earliest possible stage and to estimate the remaining useful life of structures (damage prognosis). Vibration-based damage identification procedures involve conducting repeated vibration surveys on the structure during its lifetime. Changes in identified dynamic characteristics such as modal parameters of structures are being used extensively for the purpose of condition assessment and damage identification of structures. Extensive literature reviews on damage identification methods based on changes in dynamic properties are provided in [1-4]. Operational modal analysis (OMA) has been used as a technology for estimating modal parameters of structures using output-only data, i.e., without the knowledge of input excitation [5, 6]. For civil structures, this technology is more suitable than experimental modal analysis (based on input-output data) [7] because: (1) it is usually very difficult if not impossible to measure the input excitations such as wind and traffic under operational conditions, and (2) it is expensive to perform dynamic experiments on in-situ structures using dynamic excitation equipment (e.g., shakers, actuators) allowing measurement of the excitation [8]. It should be noted that the success of vibration-based damage identification methods depends strongly on the completeness and accuracy of the identified modal parameters [9]. This study investigates systematically, based on a shear wall testbed structure, the variability of modal parameters identified using three output-only system identification methods due to the uncertainty/variability of several input factors. These input sources of variability include choices made in (*i*) the design of the dynamic tests or experiments, (*ii*) the data collection, and (*iii*) the data processing/analysis.

A full-scale, 7-story reinforced concrete (RC) shear wall building slice was tested on the NEES shake table at the University of California San Diego (UCSD-NEES shake table) during the period of October 2005 to January 2006. The shake table base excitation tests were designed to damage the building progressively through historical earthquake ground motions on the shake table. At various levels of damage, several low amplitude white noise base excitations were applied, through the shake table, to the building that responded as a quasi-linear system with modal parameters depending on the level of structural damage. Three output-only system identification methods, namely (1) Natural Excitation Technique combined with the Eigensystem Realization Algorithm (NExT-ERA) [10, 11], (2) Data-driven Stochastic Subspace Identification (SSI-Data) [12], and (3) Enhanced Frequency Domain Decomposition (EFDD) [13], were used to estimate the modal parameters (natural frequencies, damping ratios and mode shapes) of the building at its undamaged (baseline) and various damage states [14]. The variability in the system identification results was observed to be significant, which motivated the uncertainty analysis of system identification results presented in this paper. Furthermore, in an earlier study [9], the authors

performed an uncertainty analysis of the damage identification results obtained from a finite element (FE) model updating strategy applied to dynamic data simulated from a nonlinear FE model of the seven-story building structure considered here. One of the input factors of that study consisted of the level of uncertainty of the (identified) modal parameters at the undamaged and various damage states of the structure, which was found to play a significant role in the uncertainty of the damage identification results.

This study examines the performance of the above mentioned system identification methods as applied to the measured dynamic response of the building (Case I) and the dynamic response of the building simulated using a nonlinear FE model thereof (Case II). The variability of the modal parameters identified at various states of the structure due to variation of four input factors is analyzed. The simulated dynamic response of the building used in Case II was generated using a three-dimensional nonlinear finite element model of the building developed in the structural analysis software framework OpenSees [15]. A full factorial design of experiments is used in each case, thus considering all possible combinations of the input factors. Analysis-of-variance (ANOVA) [16, 17] is employed to quantify the variability of the identified modal parameters due to variation of the input factors. In addition to ANOVA, meta-models [18, 19] are used for effect screening in Case II (based on the simulated dynamic response data). The meta-models considered also include the effects of linear interactions of the input factors.

2. Test Specimen, Instrumentation and Dynamic Experiments

The test structure represented a section/slice of a full-scale seven story reinforced concrete wall building and consisted of a main wall or web wall, a back wall or flange wall perpendicular to the main wall providing transversal stability, concrete slabs at floor levels except at the base, a post-tensioned auxiliary column providing torsional stability, and four gravity columns transferring the floor slabs weights to the shake table. Slotted slab connections located between the web and flange walls at floor levels allow the transfer of in-plane diaphragm forces while minimizing the moment transfer between the web and flange walls. Figure 1 shows the test structure mounted on the shake table. More details about the test structure can be found in [20]. Mechanical and dynamic characteristics of the shake table and its controller are available in [21].

The test structure was instrumented with a dense array of strain gages, accelerometers, linear variable displacement transducers (LVDTs), and potentiometers from which data were simultaneously sampled using a nine-node distributed data acquisition system. In this study, data from 28 longitudinal acceleration channels - three located at each floor level and one at mid-height of the web wall at each story - were used for identifying the effective modal parameters at different undamaged and damaged states of the test

structure. The acceleration responses were measured at a rate of 240Hz resulting in a Nyquist frequency of 120Hz, which is higher than the frequencies of interest in this study (< 25Hz). More details about the instrumentation layout are available in [14].

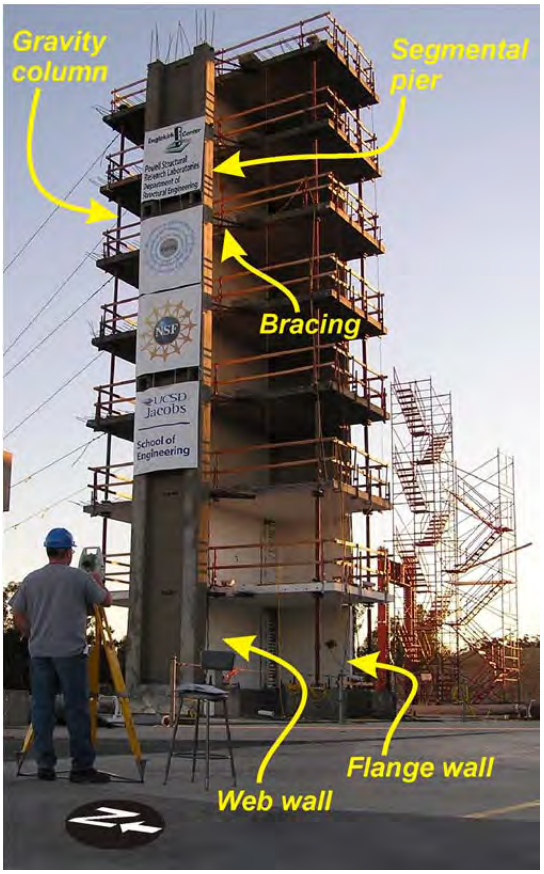

Figure 1. Test structure

A sequence of 68 dynamic tests was applied to the test structure including ambient vibration tests, forced vibration tests (white noise and seismic base excitations), and free vibration tests. The building was damaged progressively through four historical earthquake ground motions, and the modal parameters of the building at various damage states were identified using different system identification methods and different test data. As already mentioned, the observed variability in the system identification results motivated the authors to perform an uncertainty analysis. The uncertainty analysis study presented in this paper is based on the measured data from an ambient vibration test and two banded white noise (0.25-25Hz) base excitation tests with root mean square (RMS) amplitudes of 0.03g and 0.05g, all performed after the application of the first earthquake and before the building was exposed to the second earthquake. The maximum length of measured data for each of the three tests is 3 minutes. The first earthquake

ground motion applied to the building was the longitudinal component of the 1971 San Fernando earthquake at the Van Nuys station (M_w = 6.6).

In addition to the uncertainty analysis based on the experimentally measured data, another case of analysis is performed based on the FE simulated response of the building obtained from a calibrated nonlinear FE model thereof. This numerical study allows investigating the effect of added measurement noise as another input factor and also comparing the system identification results with the "exact" eigenvalues of the damaged FE model of the structure after application of the gravity loads.

3. Finite Element Response Simulation

A three dimensional nonlinear finite element model of the structure was developed using the software framework OpenSees for advanced modeling and simulation of structural and/or geotechnical systems with applications in earthquake engineering [15]. The FE model is composed of 509 nodes, 233 beam-column elements and 315 linear elastic shell elements. Both the web (in the East-West direction) and flange (in the North-South) walls are modeled as force-based nonlinear beam-column elements with fiber cross-sections and with the Euler-Bernoulli kinematic assumption (i.e., beam/column cross-sections remain plane and perpendicular to the centroidal axis in the deformed configuration). These elements allow the spread of plasticity along the height of the walls. Recent years have seen great advances in the nonlinear analysis of frame structures. Advances were led by the development and implementation of force-based elements, which are superior to classical displacement-based elements in tracing material nonlinearities such as those encountered in reinforced concrete beams and columns [22, 23]. Displacement-based beam-column elements are based on the interpolation of the displacement fields along the element (typically cubic Hermitian polynomials for the transverse displacement, which are exact only for linear elastic prismatic beam-column). This interpolation becomes an approximation when the element is not prismatic and/or the material is nonlinear. Therefore, for nonlinear analysis, displacement-based beam-column elements provide only an approximate solution, the accuracy of which can be improved by increasing the number of elements used to model each beam/column of the structure. Force-based elements are based on the interpolation of the internal force fields along the element, which is exact (i.e., satisfies equilibrium exactly). This interpolation is exact whether the element is prismatic or not, linear or nonlinear. Therefore, the formulation of the force-based element is exact irrespective of the variation of the beam cross-section properties over its length and the state of the material (linear, nonlinear). The fiber cross-sections are defined from the cross-sectional geometry, longitudinal reinforcement bars, and material properties of the walls. For each story, the web wall is discretized into four elements, and four Gauss-Lobatto integration points are used along the length of each element. Figure 2 shows the discretization of the web wall using force-based fiber-section nonlinear beam column

elements, the fiber discretization of the wall cross-section, and the uni-axial constitutive laws adopted for the concrete (unconfined and confined) and steel material/fibers. Figure 2(a) shows the first-story web wall discretization into four elements with four Gauss-Lobatto integration points each. At the first story, the fiber cross-section of the web wall (with two layers of reinforcing steel at both ends of the walls) contains the following sub-regions as shown in Figure 2(b): one region at each end (East and West) of the wall containing confined concrete; one region near the West end also containing confined concrete but with a lesser level of confinement; and the cover and central regions containing unconfined concrete. As shown in the plot, a total of 16 #5 (i.e., with nominal diameter of 5/8 inch or almost 16 mm) and 13 #4 (i.e., with nominal diameter of 4/8 of an inch or almost 13mm) reinforcing steel bars are used in the longitudinal (vertical) direction, while #4 bars spaced at 203 mm (8 inch) on center are used for the transverse (horizontal) reinforcement. From the second to the top story, the entire cross-sections of both the web and flange walls (each with a single central layer of reinforcing steel) are modeled with unconfined concrete material. The uni-axial stress-strain constitutive laws for unconfined and confined concrete fibers (with two different levels of confinement) and the steel fibers (rebars) are illustrated in Figure 2(c). All the longitudinal reinforcing steel bars are discretized at the locations specified on the construction drawings. The OpenSees material type *Concrete04* is used to model both the unconfined (cover) and confined concrete regions of the wall cross-sections. This uni-axial concrete material constitutive model is based on the modified Kent-Park model to represent the concrete compressive stress-strain curve, enhanced by using the pre- and post-peak curves proposed by Popovics in 1973 [15]. The unloading and reloading stress-strain characteristics are based on the work of Karsan and Jirsa [24]. Tensile capacity and softening are also specified for the concrete material models used in the FE model. The properties of the confined concrete fibers are determined according to Mander's model [15]. The deformed mild steel reinforcement is modeled using the OpenSees *Steel02 material model* corresponding to the Menegotto-Pinto model which is able to reproduce the Bauschinger effect [25]. The fiber section properly accounts for the nonlinear material coupling between the axial and bending behaviors, and the assumed linear-elastic shear force-deformation behavior is aggregated at the section level in a materially uncoupled way. Shear behavior is coupled to the bending behavior only at the element level through equilibrium. For more details about the underlying theory of the FE and material models used, the interested reader is referred to the OpenSees User's Manual [15].

The gravity columns, braces and post-tensioned column are assumed to remain linear elastic during the analyses, so they are modeled as linear elastic elements. For the same reason, the slabs are also modeled as linear elastic shell elements. The slotted slab connections between the two walls are modeled using shell elements with reduced thickness. All tributary masses and corresponding gravity loads are applied to the nodes at floor levels. Rayleigh damping is assigned to the model by matching a damping

ratio of 2.5% at the frequencies 2Hz and 10Hz, which is consistent with the results of previous system identification studies performed on this structure [14]. During each dynamic response analysis, the gravity loads are first applied to the model quasi-statically followed by the rigid-base excitation, which is applied dynamically. As base excitation, three base acceleration time histories are generated as Gaussian banded white noise processes (between 0.25Hz and 30Hz) with root mean square accelerations of 0.03g, 0.06g and 0.09g, respectively, where g denotes the acceleration of gravity. The implicit Newmark integration procedure with a time-step of 1/120 second (sec) is used as time integration scheme. The longitudinal acceleration response histories are recorded at the 28 nodes corresponding to the sensor locations on the test structure (i.e., three accelerometers at each floor level and one at mid-height of the web wall at each story).

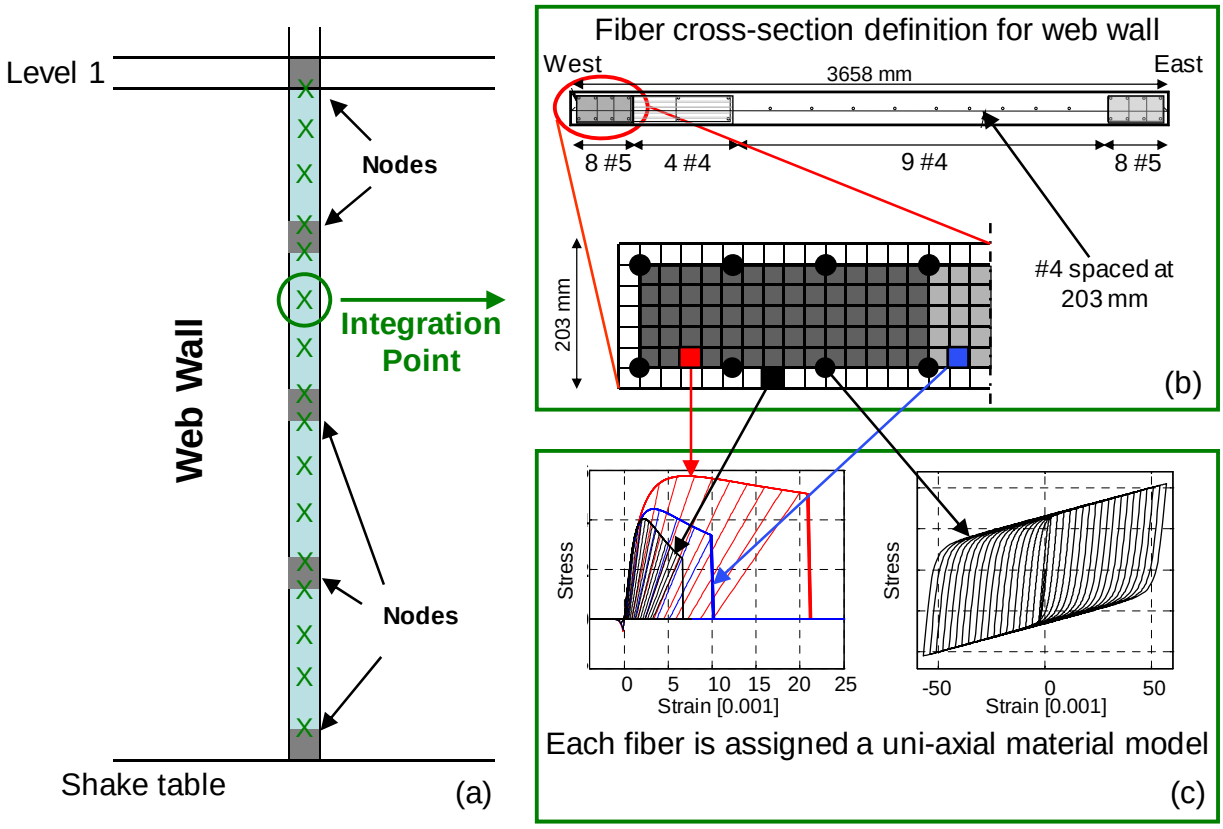

Figure 2. Wall modeling using forced-based fiber-section nonlinear beam-column elements: (a) web wall discretization at the first story, (b) sub-regions of the wall cross-section with different levels of confinement of the concrete (no confinement: white, moderate confinement: light grey, and high confinement: dark grey background), and (c) uni-axial constitutive laws for unconfined and confined concrete and steel reinforcement

The first three longitudinal mode shapes together with their corresponding natural frequencies and damping ratios are shown in Figure 3. These mode shapes and natural frequencies were computed based on the tangent stiffness matrix (after application of the gravity loads) and are in good agreement with those identified experimentally from the ambient vibration data of the undamaged test structure (see Table 1). It is worth noting that the higher natural frequency of the first mode in Case II corresponds to the FE model with uncracked concrete properties, while its counterpart from Case I was identified from the specimen with cracked concrete condition. The nonlinear FE model of the test structure was validated by comparing the simulated acceleration and displacement response time histories with their experimental counterparts for the same seismic input motions reproduced on the shake table. The FE predicted peak roof displacements closely match the corresponding experimental results for the four historical earthquake ground motions used in the shake table tests.

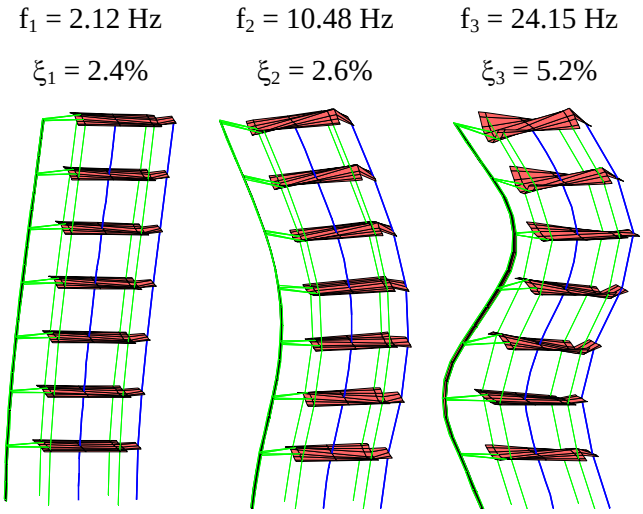

Figure 3. First three longitudinal mode shapes of FE model of test structure based on uncracked concrete properties

4. Description of Input Factors Studied and Design of Experiments

The objective of this study is to analyze and quantify the variability of the modal parameters obtained using three output-only system identification methods due to the variability of the following input factors: (1) excitation amplitude (A), (2) spatial density of the sensors (S), (3) length of structural response records used for system identification (L), (4) model order used in the parametric system identification methods (NExT-ERA and SSI-Data) (O), and (5) level of measurement noise (N) which could only be considered in the numerical study (Case II). Selection of these factors is based on previous experience of the authors in system identification of large-scale civil structures [14, 26-28]. The input factors are described in more details in the following subsections.

Table 1. Statistics of the identified modal parameters (COV = coefficient-of-variation)

		Case I		Case II		
		Mean	COV [%]	Exact	Mean	COV [%]
Natural Freq. [Hz]	Mode 1	1.67	12.0	2.12	1.94	9.8
	Mode 2	11.16	3.8	10.48	10.01	4.4
	Mode 3	-	-	24.15	21.33	3.1
Damping Ratio [%]	Mode 1	4.9	71.4	2.4	5.2	59.6
	Mode 2	4.2	71.4	2.6	2.6	65.4
	Mode 3	-	-	5.2	3.2	59.4
MAC	Mode 1	0.95	8.4	1	0.96	17.7
	Mode 2	0.89	12.4	1	0.99	5.1
	Mode 3	-	-	1	0.93	11.8

4.1. Excitation Amplitude

The three system identification methods considered in this study provide estimates of the modal parameters of a linear structure. These methods are based on linear system theory. In the case that they are applied to nonlinear response measurements, the modal parameter estimates are to be interpreted as equivalent or effective linear modal parameters. Reinforced concrete structures are highly nonlinear, with nonlinearities staring at low amplitude excitation. The level of structural response nonlinearity is directly related to the amplitude of the input excitation. To study the performance of these system identification methods as applied to nonlinear structural data, the response of the building is considered at three levels of input excitation. In Case I (based on measured experimental data), the three levels of excitation are: (1) ambient excitation, (2) 0.03g RMS banded (between 0.25Hz and 25Hz) white noise base excitation, and (3) 0.05g RMS banded white noise base excitation. The three levels of input excitation in Case II (based on FE simulated data) are 0.03g, 0.06g, and 0.09g RMS banded (between 0.25Hz and 30Hz) white noise base excitation. Figure 4 plots the coherence function between the base input excitation (i.e., table acceleration) and the roof acceleration response for both cases of measured and simulated data and for different levels of white noise base excitation. The coherence function could not be computed for the ambient vibration test data in Case I since the input excitation is unknown and therefore unmeasured. From this figure, it can be seen that the response nonlinearity increases with increasing level of base excitation. This is consistent with the (simulated) moment-curvature hysteretic response at the base of the web wall in which the plastic curvature increases significantly as the RMS of the white noise base acceleration increases from 0.03g to 0.09g. In Figure 4, it is also observed that at the same amplitude of

base excitation (0.03g RMS), nonlinearity in the measured (experimental) response is larger than that in the simulated response. This can be due to more noise in the test data and/or other sources of nonlinearity in the test data such as rattling of loose connections from the slackness between the nut and the threaded rod in gravity columns (1.5mm of slackness) when they go from compression to tension or vice versa, and the slack at both ends of the steel braces connecting the post-tensioned column to the floor slabs. Figure 5 shows the roof acceleration response time histories and their power spectral densities for the two base excitations (0.03g and 0.05g RMS) in Case 1. It is observed that the peak of the power spectral density decreases as the excitation amplitude increases. This indicates that the first natural frequency decreases with increasing excitation amplitude due to system nonlinearity (softening).

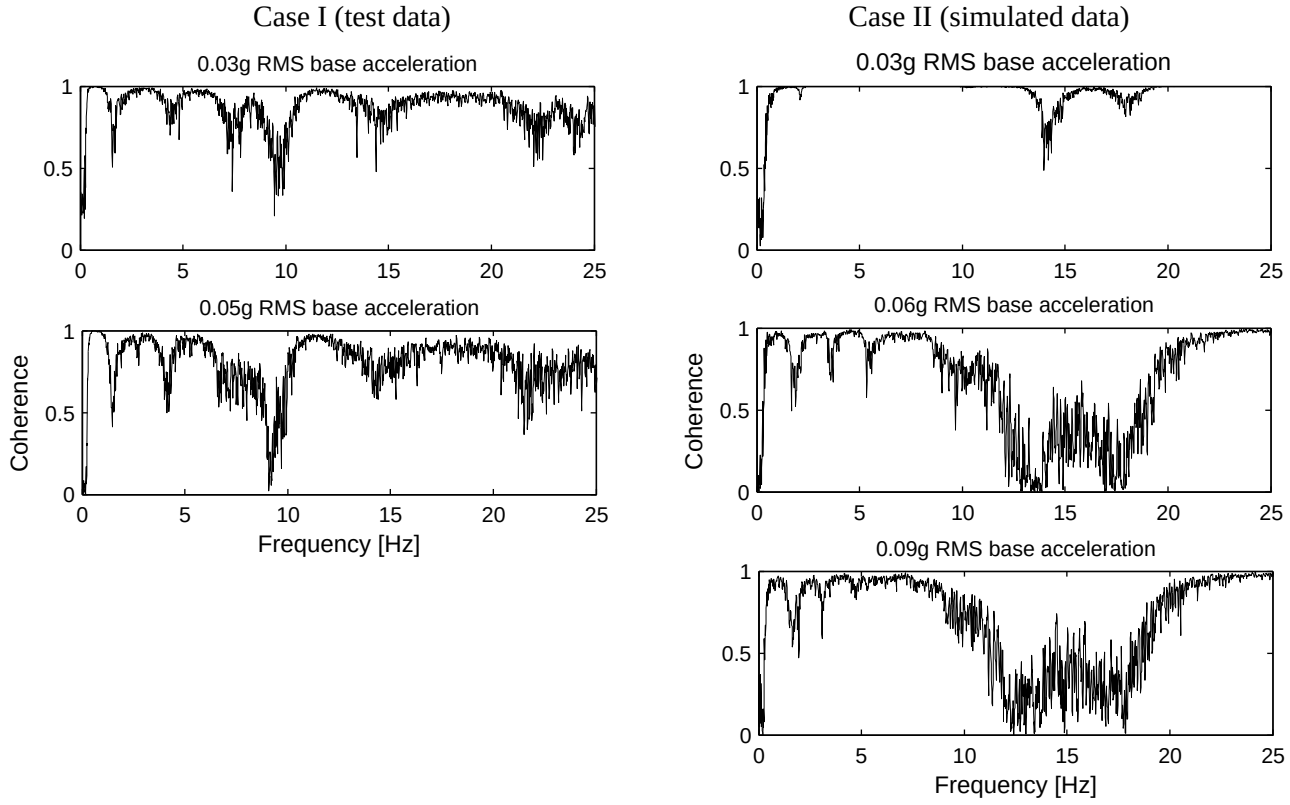

Figure 4. Coherence functions between base input (table acceleration) and roof acceleration response for Cases I and II and different levels of base excitation

4.2. Spatial Density of Sensors

An instrumentation array of 28 uni-axial acceleration channels is used during the shake table tests to measure the response of the structure in the base excitation direction (East-West). The same array of acceleration response histories is simulated using the nonlinear FE model of the structure in OpenSees. This array of 28 acceleration channels consists of three channels on each floor slab (at the north end, in the middle, and at the south end) and one channel on the web wall at mid-height of each story. To study

the performance of the system identification methods as a function of the spatial density of the sensor array (i.e., number of sensors), three different subsets of the 28 sensor array are considered. The configuration of accelerometers in each of these three subsets is: (1) seven accelerometers on the web wall at floor levels (i.e., top of each story wall), (2) fourteen accelerometers on the web wall at floor levels and mid-height of each story, and (3) full array of twenty eight accelerometers.

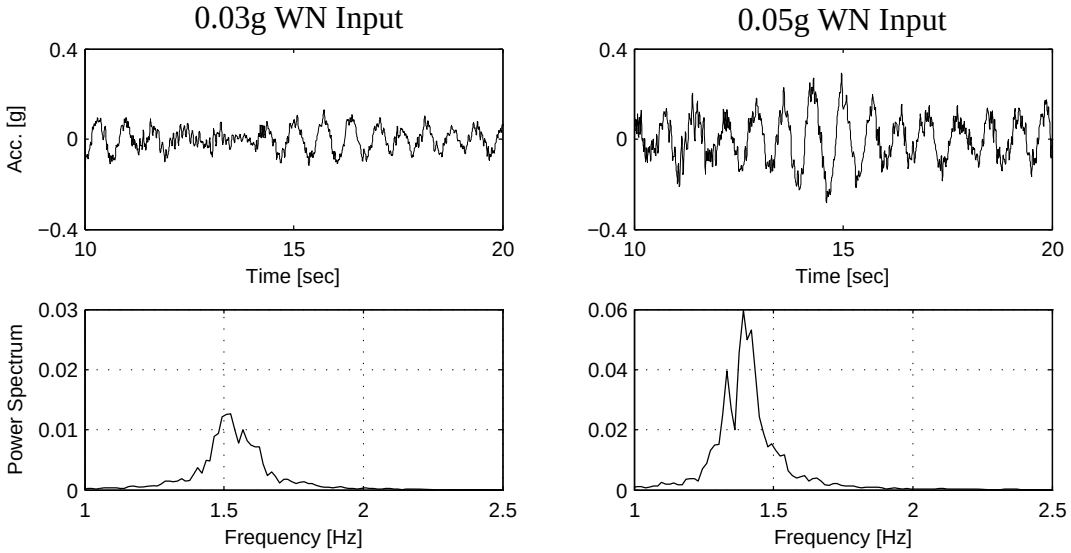

Figure 5. Roof acceleration responses and their power spectral densities for 0.03g RMS (left) and 0.05g RMS (right) white noise base excitations

4.3. Length of Structural Response Records Used for System Identification

Three different lengths of measured or simulated structural dynamic response data are considered in each of the two cases, namely: (1) 30 sec, (2) 60 sec, and (3) 180 sec. It should be noted that in many practical applications of OMA, longer durations of structural ambient vibration response (up to 1,000 times the fundamental period) are used in the identification process to ensure that an adequate level of estimation accuracy is achieved. However, this study focuses on a wide range of system identification cases, including some extreme cases where the OMA methods are challenged, i.e., when the available data is short and/or data is nonlinear such as in the case of small or moderate amplitude earthquakes. This input factor and its levels are selected based on the authors' previous experience and the available experimental data.

4.4. Model Order

When using parametric linear system identification methods for obtaining equivalent modal parameters of nonlinear systems, the order of the equivalent linear system can be a source of estimation variability or uncertainty. Since the instantaneous modal parameters are functions of the structure tangent

stiffness matrix, they vary as the latter changes during the response history. Therefore, the Frequency Response Functions (FRF) estimated from the data will not have narrow resonant peaks at the equivalent modal frequencies even in the case of noise-free data. With increasing order of the equivalent linear system, a larger number of modes are used to fit the cluster of peaks around each vibration mode, which results in variability in the identified natural frequencies and especially damping ratios. In this study, to investigate the effect of model order on the identified damping ratios, two model orders of 12 (fitting the data with maximum of 6 physical modes) and 24 (fitting the data with maximum of 12 physical modes) are considered. The model orders of 12 and 24 are selected such that the vibration modes of interest are stabilized in the stabilization diagram even for the most challenging identification cases. The vibration modes of interest are the first two longitudinal modes in Case I and the first three longitudinal modes in Case II and are selected using the Modal Assurance Criterion (MAC) metric [29]. Identified modes are selected to have the largest MAC value with the corresponding exact mode shape in Case II or the most accurately identified mode shape in Case I (A = ambient vibration; S = 28 acceleration channels; L = 180 sec). It is worth noting that even when using a stabilization diagram for order selection, the modal parameter estimates depend on the selected model order, especially when the underlying system to be identified is nonlinear.

4.5. Measurement Noise

This input factor could be considered only in Case II of uncertainty analysis (based on simulated data). In this case, the measurement/sensor noise is modeled as zero-mean Gaussian white noise processes that are added to all channels of simulated acceleration response data. This type of measurement noise is commonly used to approximate unmodeled parasitic high frequency dynamics in addition to actual sensor noise [30, 31]. The noise level is defined as the ratio of the RMS of the noise process to the RMS of the noise-free acceleration response process at each channel. This ratio is kept constant at all channels for a given noise level. Two levels of measurement noise, namely 5%, and 20%, are considered here to study the effect of this input factor on the variability of the identified modal parameters. The noise processes added to all acceleration channels are assumed statistically independent. Due to the random characteristics of the added noise, for each combination of the five input factors investigated (excitation amplitude, spatial density of sensors, data length, model order, and noise level), a set of 100 system identification runs is performed based on a set of random (i.e., statistically independent) realizations of the Gaussian white noise vector process used to model the measurement noise at all acceleration response channels. Variability of the mean and standard deviation of the identified modal parameters for these 100 identification trials is investigated as a function of the input factors.

Table 2 reports the input factors and their levels for the two cases of uncertainty analysis. A full factorial design of experiment is used in this study, resulting in a total of $3\times3\times3\times2=54$ and $3\times3\times2\times3\times2\times100=10,800$ (a set of 100 identification runs are considered for each combination of input factors) identification runs for Cases I and II, respectively, and for each of the two parametric identification methods (NExT-ERA and SSI-Data). For the nonparametric method (EFDD), model order is not an input factor, therefore $3\times3\times3=27$ and $3\times3\times3\times2\times100=5,400$ identification runs are performed for Cases I and II, respectively. A design of experiments is an organized approach for setting up physical or numerical experiments. A common experimental design is a full factorial design that considers all possible combinations of the input factors at all levels. This design of experiments requires a large number of runs, but it minimizes aliasing when used for the ANOVA [16]. The 27,135 system identification runs in this study were performed in Matlab.

Table 2. Description of input factors studied and their levels considered

Factor	Description	Levels	
		Case I	**Case II**
A	Excitation amplitude	3 levels (AV, 0.03, 0.05g)	3 levels (0.03, 0.06, 0.09g)
S	Spatial density of sensors	3 levels (7, 14, 28)	3 levels (7, 14, 28)
N	Noise level	N/A	2 levels (5, 20%)
L	Length of measured data	3 levels (30, 60, 180sec)	3 levels (30, 60, 180sec)
O	Model order	2 levels (12, 24)	2 levels (12, 24)

5. System Identification

Three output-only (i.e., no information about the input excitation is used) system identification methods were used to identify the modal parameters of the test structure based on its measured or simulated response data. These methods are: (1) NExT-ERA, (2) SSI-Data, and (3) EFDD. The measured acceleration responses were sampled at 240Hz, while the acceleration responses simulated from the FE model were decimated at 120Hz. In both cases, the Nyquist frequency (120Hz or 60Hz) is much higher than the modal frequencies of interest in this study (below 25Hz). Before applying the above mentioned system identification methods to the measured and simulated data, all the absolute acceleration response time histories were band-pass filtered (0.5-25Hz in Case I and 0.5-30Hz in Case II) using a high order (1024) Finite Impulse Response (FIR) filter. Furthermore, the absolute horizontal acceleration measurements from the white noise base excitation tests were converted to relative acceleration by subtracting the base/input acceleration. It is noteworthy that these three methods are based on the

assumption that the input excitation is a broadband (ideally white noise) signal. Therefore, violation of this assumption will result in some additional modal parameter estimation errors.

A key issue in the application of NExT-ERA is the selection of the reference channel in order to avoid missing modes in the identification process due to the proximity of the reference channel to a modal node. It is worth noting that multiple reference channels can also be used in the application of NExT-ERA. Use of multi-reference channels versus a single-reference channel usually improves the system identification results in the application of automated and continuous operational modal analysis. However, with the understanding that adding a bad reference channel (close to a modal node) will pollute some of the estimated cross power spectral density functions, use of a smaller number of (even one) reference channels can provide more accurate system identification results. In this study, one reference channel provides accurate modal identification results and therefore there is no need to use multiple reference channels. The reference channel is selected based on the configuration of the sensor array considered in the identification. In the case of 7 or 14 channels, the sensor at the second floor on the web wall is selected as reference. In the case of 28 acceleration channels, one of the two channels on the second floor slabs is selected as reference. The response cross-correlation functions are estimated through inverse Fourier transformation of the corresponding cross-spectral density (CSD) functions. Estimation of the CSD functions is based on Welch-Bartlett's method using three equal length Hanning windows with 50 percent overlap. The estimated cross-correlation functions are then used to form Hankel matrices for applying ERA in the second stage of the identification process. In the implementation of SSI-Data, the filtered acceleration response data are used to form an output Hankel matrix including 25 block rows (30 block rows when using a signal length of 180 seconds) with either 7, 14 or 28 rows in each block (equal to the number of acceleration channels considered). The number of block rows multiplied by the number of measurement channels indicates the maximum model order that can be realized. Increasing the number of block rows (or reducing the aspect ratio of the Hankel matrix) usually improves the system identification results until this number is large enough, i.e., the results converge. The number of block rows in this study is selected such that (1) the largest model order considered (O = 24) can be realized and (2) increasing this number will provide negligible improvement in the system identification results. Note that all of the measured data are used in the Hankel matrix, independently of the number of block rows selected. In the application of the EFDD method, the auto/cross-PSD functions are estimated based on Welch-Bartlett's method using Hanning windows (2 to 6) of different sizes depending on the measurement length, with 50 percent of window overlap. The window lengths used in estimating the power/cross spectral density functions affect the frequency resolution and, to some extent, the accuracy of the identified modal parameters. In this study, effects of this source of variability on the modal identification results are not considered. The choice of window lengths was considered to provide a

reasonable frequency resolution for all identification cases. After estimating the auto/cross- power spectral density functions, the response PSD matrices at all discrete frequencies are each subjected to singular value decomposition. The modal parameters are then estimated as described in [13].

5.1. Identified Modal Parameters Based on Measured Data (Case I)

As mentioned above, a full factorial design of experiment is considered in this study and therefore $3\times3\times3\times2=54$ system identifications are performed using each of the NExT-ERA and SSI-Data methods, and $3\times3\times3=27$ using the EFDD method based on the measured test data in Case I. Figure 6 shows the spread of the identified modal parameters (natural frequencies, damping ratios, and MAC values between each identified mode shape and the corresponding mode shape identified using the following values of the input factors: A = ambient, S = same as the identified mode, L = 180 sec, O = 12) for the first two longitudinal modes and each of the three identification methods used. Statistics of the identified modal parameters are reported in Table 2. Figure 7 shows in box plots the distributions of the natural frequencies and damping ratios identified using all three methods for the each level of excitation amplitude. In these plots, the end of the boxes are the lower and upper quartiles of the data, i.e., $a^j_{0.25}$ and $a^j_{0.75}$. The vertical lines in the boxes are the medians $a^j_{0.5}$, and the empty circles denote the mean values. The outside bars on the right of the boxes are the minimum of $a^j_{0.75}+1.5\times(a^j_{0.75}-a^j_{0.25})$ and $a^j_{\max}$, and the outside bars on the left are the maximum of $a^j_{0.25}-1.5\times(a^j_{0.75}-a^j_{0.25})$ and $a^j_{\min}$. The observations falling outside of these bars are shown with crosses. This figure shows the significant influence of the excitation amplitude on the distributions of the identified modal parameters, especially the first natural frequency. The identified natural frequency (mean and median values) of the first mode decreases significantly with increasing level of excitation amplitude. This is due to the fact that the length of the plastic hinge developed at the bottom of the web wall is approximately 1/10th of the total height of the wall. Therefore, most of the change in the curvature of the deflected shape occurs at the bottom of the wall (in the plastic hinge region) which affects the first mode more significantly than the higher modes. The raw results shown in Figures 6 and 7 and reported in Table 2, however, do neither contain nor quantify the contribution of each input factor or combination of input factors to the total variability of the identified modal parameters.

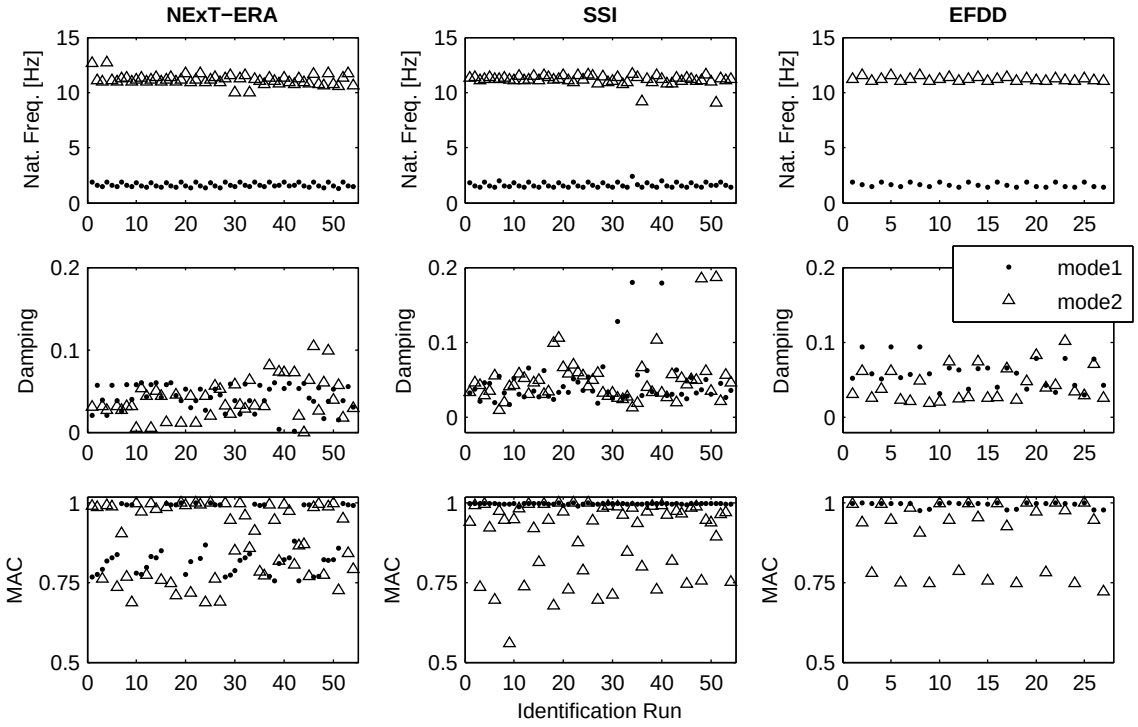

Figure 6. Identified modal parameters as a function of the input factors (Case I)

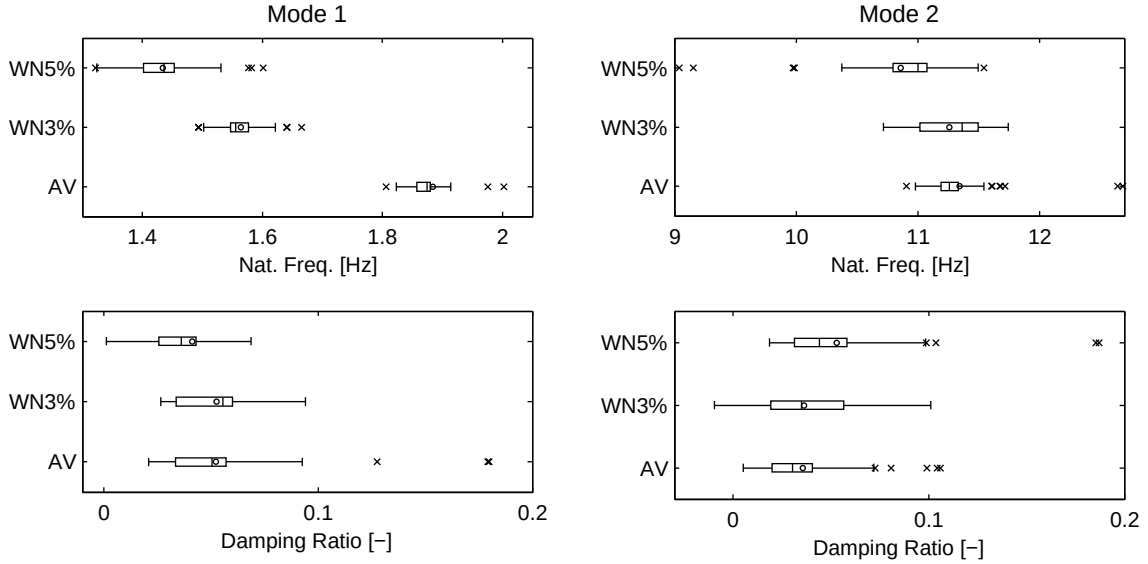

Figure 7. Distributions of identified modal parameters in box plots for different amplitudes of excitation (Case I)

5.2. Identified Modal Parameters Based on FE Simulated Data (Case II)

The spread of the modal parameters, identified based on simulated data in Case II, comes from varying the five input factors A, S, N, L, and O resulting in $3\times3\times2\times3\times2=108$ combinations thereof for the parametric methods NExT-ERA and SSI-Data and the four input factors A, S, N, and L resulting in $3\times3\times2\times3=54$ combinations thereof for the non-parametric method EFDD. Figure 8 shows the spread of the statistical mean (for each ensemble of 100 identifications) of the identified modal parameters (natural frequencies, damping ratios, and MAC values between the identified mode shapes and their nominal counterparts computed from the FE model) for the first three longitudinal modes and each of the three identification methods used. Thus, each of the points in this figure corresponds to the mean over 100 identification trials with independent vector measurement noise realizations. Reducing the set of 100 modal identification results for each combination of the input factors to the statistical mean is a crude variance reduction technique that lowers the variability of the identified modal parameters due to the choice of the vector measurement noise process (i.e., seed number of the vector noise realization). Table 1 reports the mean, standard deviation, minimum and maximum values of the statistical mean (over the 100 realizations) of the identified modal parameters. Figure 9 shows in box plots the distributions of the statistical mean (over the 100 realizations) of the identified (using all three method) modal parameters with the mean and median values (shown as an empty circle and vertical bar inside the box, respectively). From this figure, it is observed again that the excitation amplitude has a significant effect on the identified modal parameters. In general, with increasing level of excitation amplitude, it is found that the identified natural frequencies (mean and median values thereof) decrease, while the identified damping ratios (mean and median values thereof) increase, especially for the first vibration mode.

6. Uncertainty Quantification

In this section, first the analysis of variance (ANOVA) is employed to partition the observed (total) variability of the modal parameters identified using NExT-ERA, SSI-Data, or EFDD based on the measured test data (Case I) into components attributable to the sources of variability consisting here of the four input factors (i.e., excitation amplitude, spatial density of sensors, length of measured response, and model order for parametric methods NExT-ERA and SSI-Data). The second part of this section focuses on partitioning the observed (total) variability in the modal parameters identified based on the FE simulated response of the building (Case II) into contributions of the five input factors considered in this case (same as for Case I plus level of measurement noise). In the last part of this section, meta-modeling is used for effect screening of the system identification results obtained in Case II.

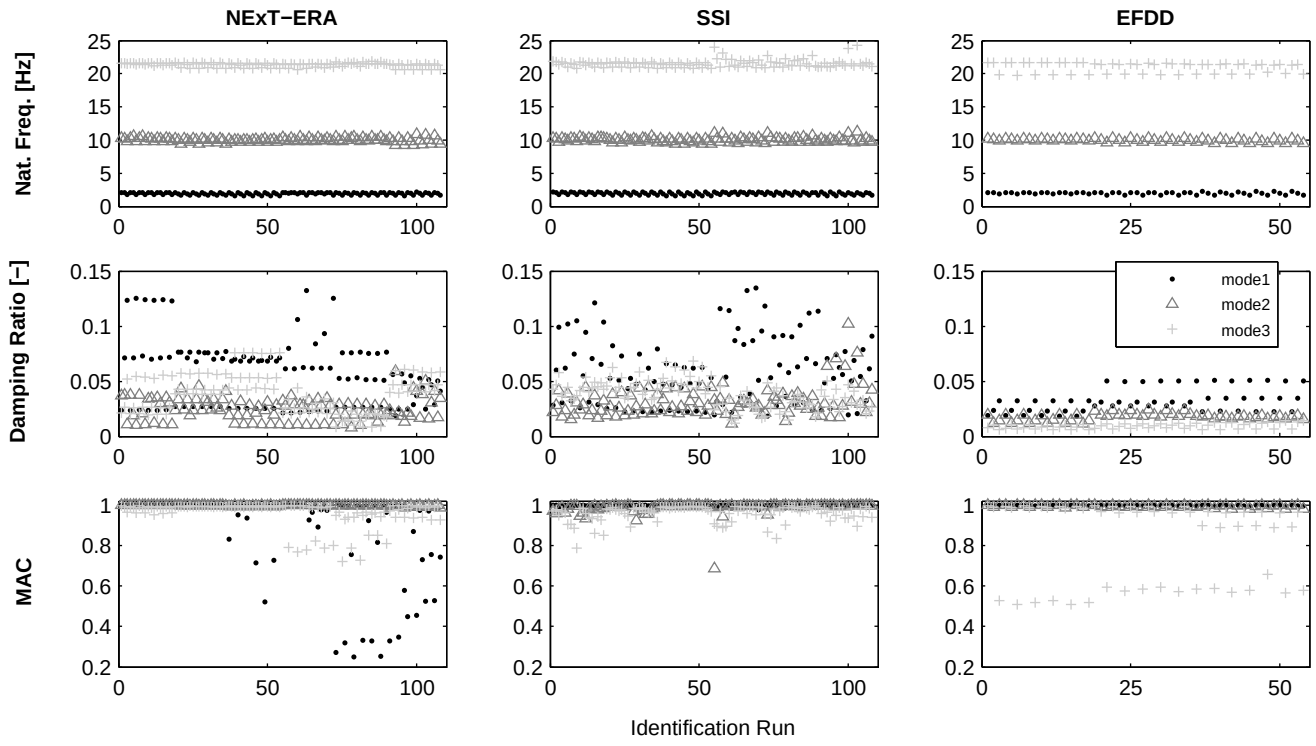

Figure 8. Statistical mean (over 100 vector measurement noise realizations) of identified modal parameters as a function of the input factors (Case II)

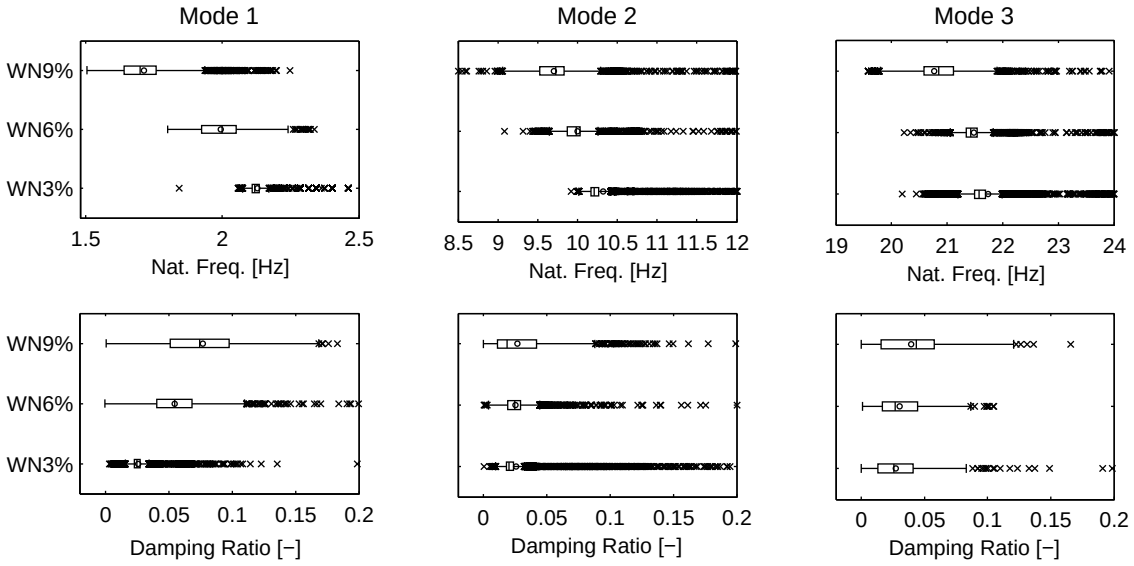

Figure 9. Distributions of statistical mean (over 100 vector measurement noise realizations) of identified modal parameters in box plots for different amplitudes of excitation (Case II)

6.1. Analysis of Variance Based on Measured Data (Case I)

To investigate the contribution of each input factor (while varying in its considered range) to the total variability of the identified modal parameters in Case I, ANOVA is performed and the obtained results are discussed. The theoretical basis of ANOVA is that the variance of output features (identified modal parameters) can be divided into correlation coefficients or partial variances, each representing the effect of an individual input factor to the total variance, independently from the others. The correlation coefficients are estimated by the R^2 values. To compute the R^2 values, the input factors **x** of the model y = *M*(**x**) are partitioned in two subsets x_f (single input factor taken as fixed or known) and $\mathbf{x}_v$ (remaining input factors assumed variable or unknown) where y denotes an output feature (identified modal parameter herein). The relative importance of input factor x_f is measured by the difference $\sigma^2(y) - \sigma^2(y|\mathbf{x}_f)$ where $\sigma^2(y)$ = unconditional variance of y, $\sigma^2(y|x_f)$ = conditional variance of y for x_f fixed. The R^2 statistic is estimated as:

$$R^2 = \frac{\sigma^2(y) - \sigma^2(y|x_f)}{\sigma^2(y)} \tag{1}$$

and represents the relative contribution of the input factor x_f to the total (unconditional) variance of the output feature, $\sigma^2(y)$. The statistic R^2 is bounded between 0 and 1, i.e., $0 \le R^2 \le 1$. A large value of R^2 indicates that the variability of the corresponding input factor controls the variability of the output feature y.

In this case, ANOVA is applied to 54 sets of modal parameters identified using NExT-ERA and SSI-Data and 27 sets of modal parameters identified using EFDD. The number of sets of identified modal parameters correspond to all the possible combinations of the four input factors based on a full factorial design of experiment. Figure 10 shows the R^2 values for the modal parameters of the first two longitudinal vibration modes (see Figure 3) identified using NExT-ERA, SSI-Data, and EFDD corresponding to the four input factors A, S, L, and O. The R^2 values are scaled such that their sum over all input factors equates 100%. From Figure 10, it is observed that: (1) factor A has the most significant influence in the variability of the modal parameters identified using all three methods, especially for the first mode natural frequency; (2) input factor L is the second most influential input factor for the first mode damping ratio identified using NExT-ERA and EFDD, while input factors S and O are more influential than L for this modal parameter identified using SSI-Data; and (3) MAC values of the first mode shape are most sensitive to input factors S and A.

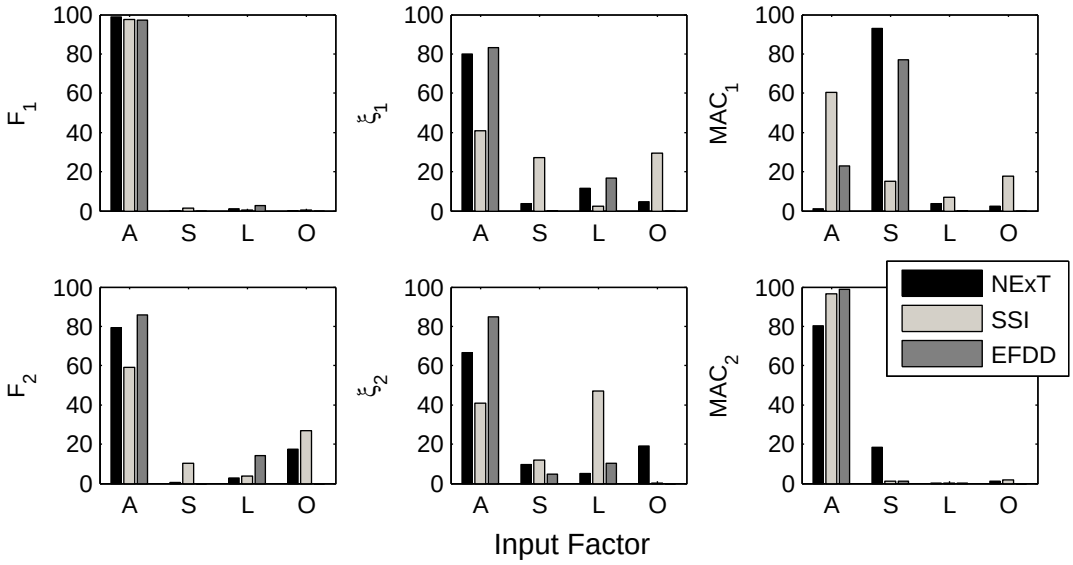

Figure 10. R^2 values of identified modal parameters due to variability of input factors A, S, L, and O (Case I)

6.2. Analysis of Variance Based on FE Simulated Data (Case II)

In this section, ANOVA is applied to 108 data sets (54 when using EFDD) of output features (mean and standard deviation of identified modal parameters for each ensemble of 100 identification trials with statistically independent vector measurement noise realizations) using a full-factorial design where the input factors are varied in the design space for each of the three system identification methods. Figure 11 shows the R^2 values (corresponding to the input factors A, S, N, L, and O) of the mean of each of the modal parameters of the first three longitudinal vibration modes identified using NExT-ERA, SSI-Data, and EFDD, respectively. Here also, the R^2 values of each output feature are scaled such that their sum over all input factors equates 100%. From this figure, it is observed that: (1) the variability of the mean value of the identified modal parameters (especially the natural frequencies) is in general most sensitive to input factor A for all three methods which is consistent with the results obtained in Case I; and (2) input factors S and N have the least effect on the mean values of the modal parameters identified using NExT-ERA and EFDD. Similarly, Figure 12 shows the R^2 values of the input factors for the standard deviation (over the 100 identification trials) of the output features. By comparing the results in Figures 11 and 12, it can be concluded that the level of measurement noise (N) is a significant source of variability for the standard deviations of the identified modal parameters (except for SSI-Data), which is not the case for the mean values of the identified modal parameters.

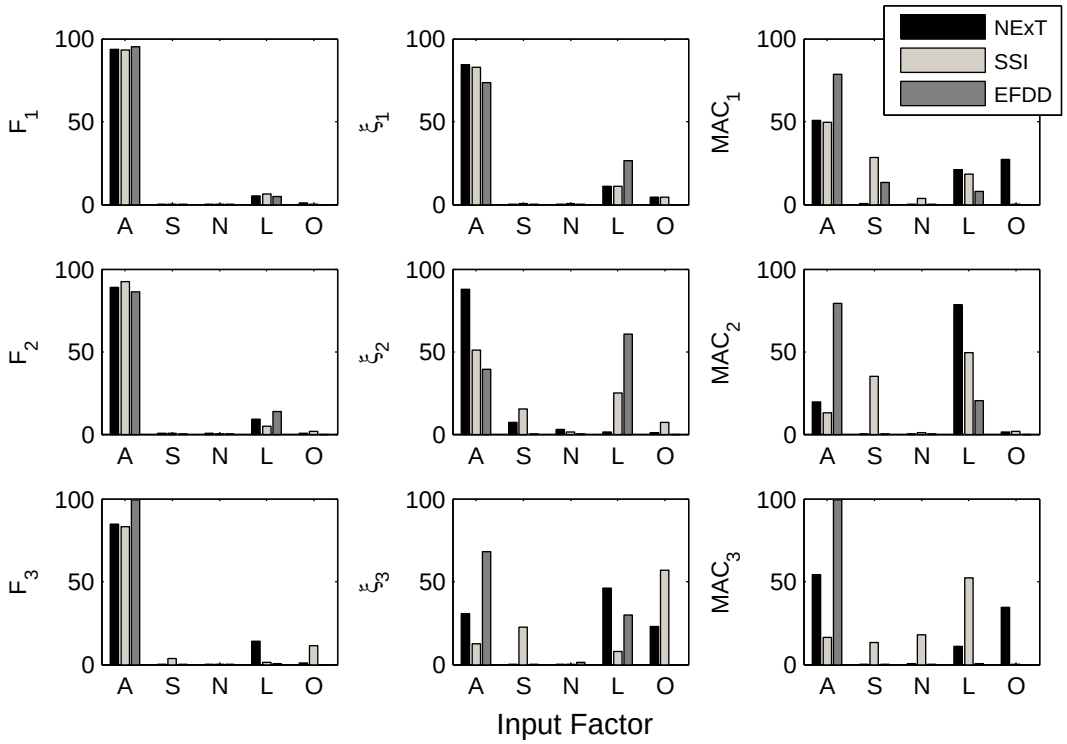

Figure 11. R^2 values of statistical mean (over sets of 100 identification runs) of identified modal parameters due to variability of input factors A, S, N, L, and O (Case II)

6.3. Meta Modeling Based on FE Simulated Data (Case II)

Meta-models also known as surrogate models are black-box numerical models (i.e., have no physical characteristics of the system) that relate the output features and the input factors. Initially, the functional forms and coefficients of meta-models must be identified which is referred to training step. The meta-model functions can include the input factors, their higher powers and their interactions. The absolute value of an input factor coefficient in a meta-model directly provides the influence of that input factor to the total variability of the output features. In order to have normalized coefficients of the input factors, the latter are scaled between -1 (corresponding to the lowest value) and +1 (corresponding to the highest value). The quality of a meta-model should be evaluated separately from the training step. In this study, the use of meta-models allows to further validate the effect screening results obtained from ANOVA. In this section, a polynomial model is fitted to the mean values of the identified modal parameters by including all input factors considered here and their linear interactions as

$$\begin{aligned} \mathrm{Y} = {} & \beta_0 + \beta_{\mathrm{A}}\mathrm{A} + \beta_{\mathrm{S}}\mathrm{S} + \beta_{\mathrm{N}}\mathrm{N} + \beta_{\mathrm{L}}\mathrm{L} + \beta_{\mathrm{O}}\mathrm{O} + \beta_{\mathrm{AS}}\mathrm{AS} + \beta_{\mathrm{AN}}\mathrm{AN} + \beta_{\mathrm{AL}}\mathrm{AL} + \beta_{\mathrm{AO}}\mathrm{AO} + \beta_{\mathrm{SN}}\mathrm{SN} \\ & + \beta_{\mathrm{SL}}\mathrm{SL} + \beta_{\mathrm{SO}}\mathrm{SO} + \beta_{\mathrm{NL}}\mathrm{NL} + \beta_{\mathrm{NO}}\mathrm{NO} + \beta_{\mathrm{LO}}\mathrm{LO} \end{aligned} \tag{2}$$

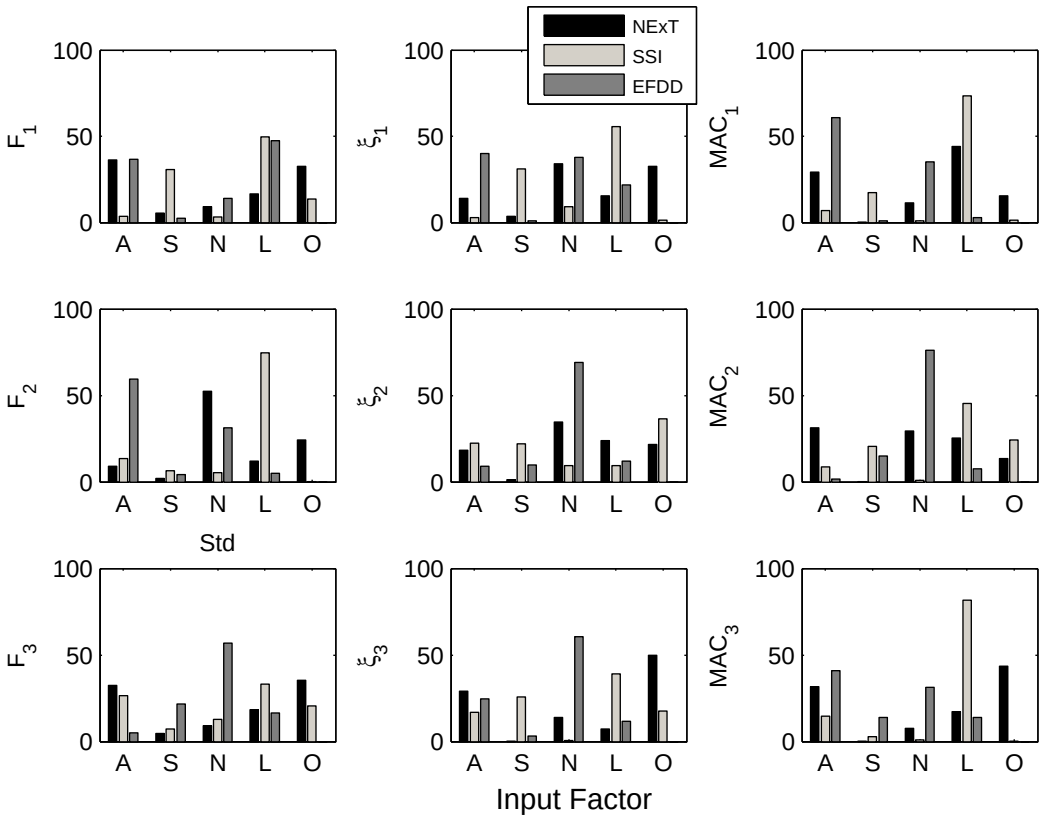

Figure 12. R^2 values of standard deviation (over sets of 100 identification runs) of identified modal parameters due to variability of input factors A, S, N, L, and O (Case II)

It should be noted that: (*i*) the identified natural frequencies and damping ratios are normalized by their nominal counterparts (computed from the FE model) so that the estimated β (regression) coefficients are all dimensionless and of the same order of magnitude for different output features; and (*ii*) the value of β_0 corresponds to the mean value of the output feature. Figure 13 shows the absolute values of the β (regression) coefficients obtained by best fitting polynomials (based on least-squares) to the mean values (over sets of 100 identification trials) of the modal parameters. The results in Figure 13 show that: (1) the identified natural frequencies are most sensitive to input factor A (as already shown by ANOVA), and then factor L and linear interaction AL; (2) in general, the identified modal damping ratios and MAC values are more sensitive to input factors S, N, and O than the natural frequencies; and (3) the variability in the considered input factors has more influence on the identified modal parameters of the first vibration mode than on those of the higher modes, i.e., the identified parameters of the first mode are more sensitive to the input factors than those of the higher modes. The last observation is consistent with the coefficients of variation of the identified modal parameters reported in Table 1 for Case II.

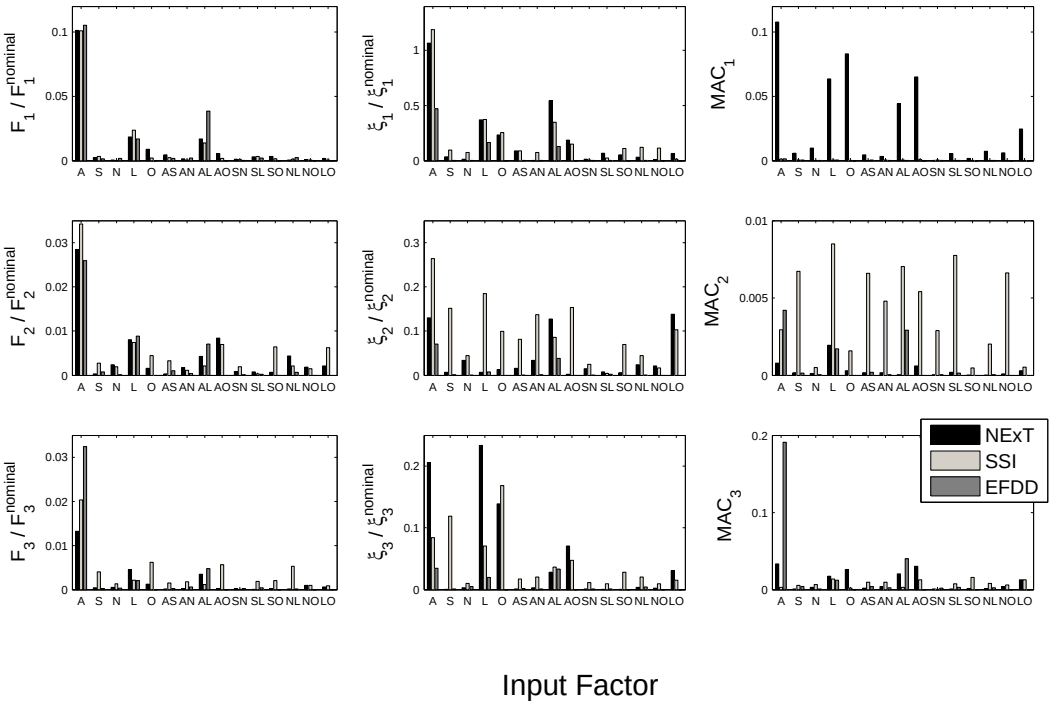

Figure 13. Absolute values of regression coefficients of best-fitted polynomial to mean values (over sets of 100 identification runs) of identified modal parameters

7. Conclusions

A full-scale, seven-story, RC shear wall building slice was tested on the NEES shake table at University of California San Diego during the period of October 2005 to January 2006. Three output-only system identification methods, namely (1) Natural Excitation Technique combined with the Eigensystem Realization Algorithm (NExT-ERA), (2) Data-driven Stochastic Subspace Identification (SSI-Data), and (3) Enhanced Frequency Domain Decomposition (EFDD), were used to extract the modal parameters (natural frequencies, damping ratios, and mode shapes) of the building specimen. In this study, an uncertainty or variability analysis of these system identification methods is performed in two cases: (Case I) when these methods are applied to the measured response of the structure, and (Case II) when these methods are applied to the response of the structure simulated using a calibrated and validated three-dimensional nonlinear finite element model thereof. The input factors considered in Case I are: (1) amplitude of input excitation (A), i.e., level of nonlinearity in the response, (2) spatial density of measurements (S), i.e., number of sensors, (3) length of the structural response data used in the identification process (L), and (4) model order used in the parametric system identification methods (O).

Case II of the uncertainty analysis also includes the measurement noise (N) in addition to the four input factors considered in Case I.

From the application of ANOVA to the system identification results based on the measured test data in Case I, it is observed that input factor A has the most significant influence on the variability of the modal parameters (especially the first mode natural frequency) identified using the three methods. In Case II of the uncertainty analysis, ANOVA is applied to the mean and standard deviation (over sets of 100 identification runs to account for the randomness of the measurement noise) of the modal parameters identified from the FE simulated data and it is observed that the variability of the mean values of the identified modal parameters (especially the natural frequencies) is in general most sensitive to input factor A for all three methods, which is consistent with the results obtained in Case I. Input factors S and N have the least effect on the mean values of the modal parameters identified using NExT-ERA and EFDD. However, the level of measurement noise (N) contributes significantly (relative to other input factors) to the variability of the standard deviations of the identified modal parameters, which is not the case for the mean values of the identified modal parameters. Meta-models are also fitted to the identified modal parameters in Case II. Based on the relative amplitudes of the β (regression) coefficients of the meta-models, it is found that the identified natural frequencies are most sensitive to input factor A (as already indicated by ANOVA), and then input factor L and linear interaction AL. It is also observed that, in general, the modal damping ratios and MAC values are more sensitive to input factors S, N, and O than the natural frequencies. The relative amplitudes of the β coefficients indicate that the considered input factors have more influence on the variability of the identified modal parameters of the first mode than on that of the higher modes.

This investigation demonstrates that the level of accuracy/confidence in the system identification results depends not only on the estimation error of the identification methods used as well as measurement noise, but also on the design of experiments (e.g., amplitude of excitation, spatial density of sensors, length of response measurement data, model order). Therefore, dynamic tests/experiments should be designed so that the most influential input factors are set at optimum (or appropriate) levels to yield more accurate (or more meaningful) system identification results.

ACKNOWLEDGEMENTS

Partial supports of this study by the Englekirk Center Industry Advisory Board and the Lawrence Livermore National Laboratory with Dr. David McCallen as program director are acknowledged. The authors would like to thank Professors Jose Restrepo, Marios Panagiotou and Ozgur Ozcelik as well as the technical staff at the Englekirk Center for their help in collecting the test data. The authors

acknowledge the support of the Engineering Institute, a joint Educational and Research Program between the University of California, San Diego, Jacobs School of Engineering and Los Alamos National Laboratory. The second author would also like to acknowledge the support provided by the Department of Civil Engineering of the Universidade Nova de Lisboa and the Portuguese Foundation for Science and Technology (BD/17266/2004). Any opinions, findings, and conclusions or recommendations expressed in this paper are those of the authors and do not necessarily reflect those of the sponsors.

REFERENCES

1. Doebling SW, Farrar CR, Prime MB. A summary review of vibration-based damage identification methods. *The Shock and Vibration Digest* 1998; 30(2): 99-105.

2. Sohn H, Farrar CR, Hemez FM, Shunk DD, Stinemates DW, Nadler BR. *A review of structural health monitoring literature: 1996-2001*. Technical Report , Los Alamos National Laboratory 2003; LA-13976-MS, Los Alamos, New Mexico, USA.

3. Carden EP, Fanning P. Vibration based condition monitoring: a review. *Structural Health Monitoring* 2004; 3(4): 355-377.

4. Cunha, A., Caetano, E., Magalhães, F. and Moutinho, C. (2013), Recent perspectives in dynamic testing and monitoring of bridges. Struct. Control Health Monit., in press.

5. Brincker R, Kirkegaard PH. Editorial for the special issue on operational modal analysis, *Mechanical Systems and Signal Processing* 2010; 24(5): 1209-1212.

6. Antonacci, E., De Stefano, A., Gattulli, V., Lepidi, M. and Matta, E. (2012), Comparative study of vibration-based parametric identification techniques for a three-dimensional frame structure. Struct. Control Health Monit., 19: 579-608.

7. Arici, Y. and Mosalam, K. M. (2005), Modal identification of bridge systems using state-space methods. Struct. Control Health Monit., 12: 381-404.

8. Peeters B, De Roeck GD. Stochastic system identification for operational modal analysis: A review. *J. of Dynamic Systems, Measurement, and Control* 2001; 123: 659-667.

9. Moaveni B, Conte JP, Hemez FM. Uncertainty and sensitivity analysis of damage identification results obtained using finite element model updating. *J. of Computer Aided Civil and Infrastructure Engineering* 2009; 24(5): 320-334.

10. James GH, Carne TG, Lauffer JP. *The Natural Excitation Technique for modal parameters extraction from operating wind turbines*. Technical Report, Sandia National Laboratories 1993, SAND92-1666, UC-261, Sandia, New Mexico, USA.

11. Juang JN, Pappa RS. An eigensystem realization algorithm for model parameter identification and model reduction. *J. Guidance Control Dyn.* 1985; 8(5): 620-627.

12. Van Overschee P, De Moore B. *Subspace identification for linear systems*. Kluwer Academic Publishers 1996; Massachusetts, USA.

13. Brincker R, Ventura C, Andersen P. Damping estimation by frequency domain decomposition. *Proc. of International Modal Analysis Conference* 2001; Kissimmee, USA.

14. Moaveni B, He X, Conte JP, Restrepo JI, Panagiotou M. System identification study of a seven-story full-scale building slice tested on the UCSD-NEES shake table. *J. of Structural Engineering, ASCE* 2011; 137(6): 705-717.

15. Mazzoni S, Scott MH, McKenna F, Fenves GL, et al. *Open system for earthquake engineering simulation - user manual (version 1.7.3)*. Pacific Earthquake Engineering Research Center, University of California, Berkeley, California, 2006.

16. Saltelli A, Chan K, Scott EM. *Sensitivity analysis*. John Wiley & Sons 2000; New York, NY.

17. Montgomery MC, Runger GC. *Applied statistics and probability for engineers*. 4th Edition. John Wiley & Sons 2007; New York, NY.

18. Wu CFJ., Hamada M. *Experiments: planning, analysis, and parameter design optimization*. John Wiley & Sons 2000; New York, NY.

19. Myers RH, Montgomery DC. *Response surface methodology*. John Wiley & Sons 1995; New York, NY.

20. Panagiotou M, Restrepo JI, Conte JP. Shake table test of a 7-Story full scale building slice - Phase I: Rectangular wall. *J. of Structural Engineering, ASCE* 2011; 137(6): 691-704.

21. Ozcelik O. *A mechanics-based virtual model of NEES-UCSD shake table: Theoretical development and experimental validation*. Ph.D. dissertation, Dept. of Structural Engineering, Univ. of California, San Diego, 2008.

22. Conte JP, Barbato M, Spacone E. Finite element response sensitivity analysis using force-based frame models. *Int. J. for Numerical Methods in Eng.*, 2004; 59(13):1781-1820.

23. Barbato M, Conte JP. Finite element response sensitivity analysis: a comparison between force-based and displacement-based frame element models. *Computer Methods in Applied Mechanics and Eng.* 2005; 194(12-16): 1479-1512

24. Karsan ID, Jirsa JO. Behavior of concrete under compressive loading. *J. of Structural Division, ASCE* 1969; 95(ST12): 2543-2563.

25. Paulay T, Priestley MJN. *Seismic design of reinforced concrete and masonry buildings*. John Wiley & Sons 1992; New York, NY.

26. He X, Moaveni B, Conte JP, Elgamal A, Masri SF. System identification of Alfred Zampa Memorial Bridge using dynamic field test data. *J. of Structural Engineering, ASCE* 2009; 135(1): 54-66.

27. Moser P, Moaveni B. Environmental effects on the identified natural frequencies of the Dowling Hall Footbridge. *Mechanical Systems and Signal Processing* 2010; 25(7): 2336-2357.

28. Moaveni B, Stavridis A, Lombaert G, Conte JP, Shing PB. Finite element model updating for assessment of progressive damage in a three-story infilled RC frame. J. *of Structural Engineering, ASCE* 2013, in press.

29. Allemang R J, Brown DL. A correlation coefficient for modal vector analysis. *Proc. of 1st International Modal Analysis Conference* 1982, Bethel, Connecticut.

30. Paganini F. A set-based approach for white noise modeling. *IEEE Transactions on Automatic Control* 1996; 41(10): 1453-1465.

31. Fekri S, Athans M, Pascoal A. Issues, progress and new results in robust adaptive control. *Int. J. Adapt. Control Signal Process.* 2006; 20(10): 519-579.